

# Phosphorus-Doped p-Type ZnO Nanorods and ZnO Nanorod p–n Homojunction LED Fabricated by Hydrothermal Method

Xuan Fang,<sup>†,‡</sup> Jinhua Li,<sup>‡</sup> Dongxu Zhao,<sup>\*,†</sup> Dezhen Shen,<sup>†</sup> Binghui Li,<sup>†</sup> and Xiaohua Wang<sup>‡</sup>

Key Laboratory of Excited State Processes, Changchun Institute of Optics, Fine Mechanics and Physics, Chinese Academy of Sciences, 16 East Nan-Hu Road, Open Economic Zone, Changchun 130033, People's Republic of China, and School of Science, Changchun University of Science and Technology, 7089 Wei-Xing Road, Changchun 130022, People's Republic of China

Received: July 01, 2009; Revised Manuscript Received: October 14, 2009

Phosphorus-doped ZnO nanorods and ZnO nanorod homojunctions were prepared by a hydrothermal method. The structural and photoluminescent (PL) characterizations showed the P atoms doped into the ZnO crystal lattice. In low-temperature PL spectra the emission peaks located at 3.310 and 3.241 eV were observed, which could be attributed to a conduction band to the phosphorus-related acceptor transition and a donor–acceptor pair transition, respectively. ZnO homojunctions were synthesized by P-doped ZnO nanorods grown on undoped ZnO nanorods. The current–voltage ( $I$ – $V$ ) measurement based on the ZnO nanorod p–n homojunctions showed a typical semiconductor rectification characteristic with a turn-on voltage of about 3.14 V, which meant the conductivity of the P-doped ZnO nanorod might be a p-type conductivity. The electroluminescence was observed at room temperature for this homojunction, which contained a violet-blue emission and a broad visible band emission.

## Introduction

ZnO, with a high exciton binding energy (60 meV) and a large band gap (3.37 eV at room temperature), is an important wide band gap semiconductor for the potential applications in short wavelength light emission diodes (LEDs), laser diodes (LD), and photodetectors. For practical device applications, durable and reproducible p-type ZnO is essential.<sup>1</sup> By now, most efforts to grow p-type ZnO materials have been focused on the fabrication of thin films. Many dopants, such as nitrogen,<sup>2</sup> phosphorus,<sup>3</sup> arsenic,<sup>4</sup> and antimony<sup>5</sup> were used to obtain p-type ZnO films.

In recent years, one-dimensional (1D) ZnO nanostructures, including nanotubes,<sup>6,7</sup> nanowires,<sup>8</sup> and nanorods,<sup>9</sup> have been studied extensively for their unique properties and potential applications in nanodevices.<sup>10,11</sup> Compared with thin films, ZnO nanostructures have prominent advantages. Almost each ZnO nanostructure is single crystal. And by using seeds, layered ZnO nanostructures could be vertically grown on different substrates. Due to these characteristics ZnO nanostructures are assumed a promising material for fabricating LEDs. p-type ZnO nanostructures have been obtained by direct growth method, such as chemical vapor deposition (CVD),<sup>12</sup> pulsed-laser deposition (PLD),<sup>13</sup> thermal evaporation,<sup>1,14</sup> and diffusion method.<sup>15</sup> Electroluminescence from ZnO nanowire p–n homojunction was observed by several groups.<sup>16,17</sup> In a recent report the conductivity of ZnO nanorods could be controlled by the seed layer in a hydrothermal growth process; p-type ZnO nanorods could be obtained on a zinc acetate derived seed layer prepared at 200 °C. And different LEDs have been fabricated on the basis of these p-type ZnO nanorods.<sup>18</sup> But it may be difficult to control the resistance and hole concentration of p-type ZnO nanostructures

only by the seed layer method. To improve this method, doping is the best choice. Until now, there has been no report about hydrothermal method growth of p-type doping ZnO nanostructures.

The hydrothermal method is considered a simple, convenient, inexpensive, and environmentally friendly method to grow ZnO nanostructures at low growth temperature. To realize p-type doping in ZnO, ammonium dihydrogen phosphate was used as one of the source materials. Then phosphorus-doped ZnO nanorods were fabricated by the hydrothermal method. After being annealed, p-type ZnO nanorods were obtained.

## Experimental Section

Before ZnO nanorod growth, a 100 nm thick ZnO film with (002) orientation was deposited on an n-type Si (100) substrate by magnetron sputtering serving as a seed layer.

**Synthesis of P-Doped ZnO Nanorods.** A 0.01 M amount of zinc acetate [ $\text{Zn}(\text{Ac})_2 \cdot 2\text{H}_2\text{O}$ ], 0.01 M hexamethylenetetramine, and 0.002 M  $\text{NH}_4\text{H}_2\text{PO}_4$  were dissolved in aqueous solution (Milli Q, 18.2 M $\Omega$  cm) to form a 50.0 mL solution. Then the above 30 mL mixed solution were transferred to a Teflon-lined stainless autoclave of 50 mL capacity. The as-grown ZnO film/Si substrate was put into the solution. The tank was conducted in an electric oven at 100 °C for 24 h. After reaction, the sample was washed by deionized water and dried in air at 60 °C for several hours. At last, the sample was annealed at 800 °C for 1 h under ambient Ar. For comparison, undoped ZnO nanorods were also grown following the same procedure without adding  $\text{NH}_4\text{H}_2\text{PO}_4$ .<sup>9</sup>

**Preparation of ZnO Nanorod p–n Homojunctions.** The 1D homojunctions were prepared by growing the P-doped ZnO nanorods on the undoped n-type ZnO nanorods under the same condition as mentioned above. But, to reduce the interspaces between nanorods (to make the electrode conveniently), we changed the concentrations of solution from 0.01 to 0.1 M for zinc acetate and hexamethylenetetramine with the required

\* To whom correspondence should be addressed. Tel.: +86-431-86176322. Fax: +86-431-4627031. E-mail: dxzhao2000@yahoo.com.cn.

<sup>†</sup> Chinese Academy of Sciences.

<sup>‡</sup> Changchun University of Science and Technology.

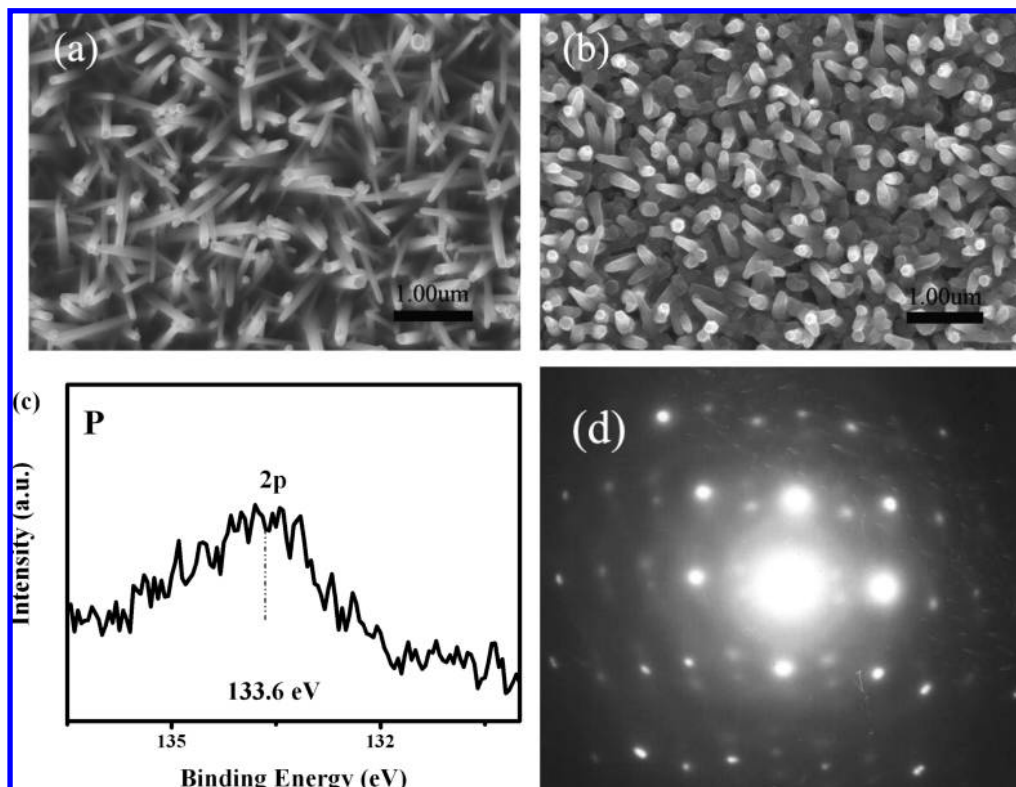


**Figure 1.** (a, b) SEM images of undoped ZnO nanorods and phosphorus-doped ZnO nanorods. (c) XPS spectrum of annealed P-doped ZnO nanorods. (d) SAED image of annealed P-doped ZnO nanorods.

amount of  $\text{NH}_4\text{H}_2\text{PO}_4$ . At last, the sample was annealed at 800 °C for 1 h under ambient Ar. Ohmic contacts were fabricated simply by sputtering In and Ni–Au/In on n-ZnO nanorods and p-type ZnO nanorods.

The morphology and structure properties of samples were investigated by field-emission scanning electron microscopy (FESEM, Hitachi-4800), energy-dispersive X-ray spectroscopy (EDS, GENE SIS 2000 XMS 60S, EDAX, Inc.) attached to the SEM, transmission electron microscopy (TEM), and a D/max-RA X-ray spectrometer (Rigaku). Photoluminescence (PL) measurements were performed using a He–Cd laser line of 325 nm as the excitation source. Electroluminescence (EL) measurements were performed by a fluorescence meter (F4500 Hitachi). The current–voltage ( $I$ – $V$ ) curve was measured by a semiconductor parameter analyzer with a sensitivity of 0.1 pA.

## Results and Discussion

The morphologies of the as-grown undoped ZnO nanorods and P-doped ZnO nanorods were characterized by using FESEM. Figure 1a shows ZnO nanorods with well-defined facets on the coated Si substrate. The nanorods have a typical diameter of about 100 nm and a length of a few micrometers. Figure 1b shows rough and uniform P-doped ZnO nanorods. The diameters of the nanorods range from 100 to 120 nm, and their lengths range from 300 to 500 nm. After the as-grown sample was annealed at 800 °C for 1 h, the morphology of the doped ZnO nanorods was almost not changed (not shown in the paper). The composition analysis detected in the energy dispersive X-ray diffraction (EDX) spectrum suggests that the P atom ratio in the nanorods is approximately 1.8% for the as-grown sample but drops to 0.6% after annealing. Because of the limit of EDX analysis, we also did an X-ray photoelectron spectroscopy (XPS) experiment to confirm the existence of P in the annealed sample (shown in the Figure 1c). The photon

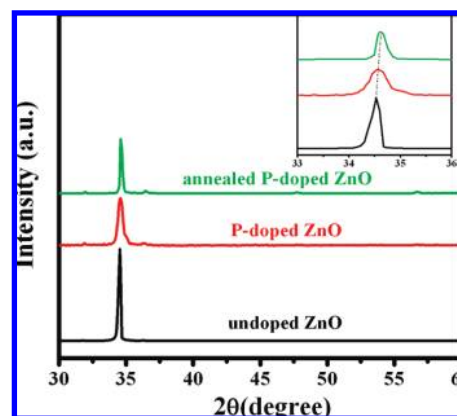


**Figure 2.** XRD pattern of the undoped ZnO nanorods and P-doped ZnO nanorods. The insert shows the amplified spectra for (002) diffractive peaks.

emission peak related to the P (2p) is observed located at 133.6 eV, which agrees well with the previous reports for P-doped ZnO.<sup>19</sup> The XPS result clearly shows that the annealed nanorods sample contains P with an atom ratio of 0.8%. The selective area electron diffraction (SAED) pattern of a single doped nanorod (annealed) is shown in Figure 1d, which confirms the P-doped ZnO nanorod is single-crystalline with the ZnO wurtzite structure.

To investigate whether phosphorus doped into the ZnO crystal lattices, the XRD measurement was performed for the undoped and doped samples. Figure 2 shows the XRD pattern of undoped ZnO and P-doped ZnO nanorods. For each sample, all the observed diffractive peaks could be indexed as the ZnO wurtzite structure. The ZnO (002) diffraction peak is dominant in the spectra, which means the samples have a preferred orientation along the  $c$ -axis. Compared with undoped ZnO, the (002)

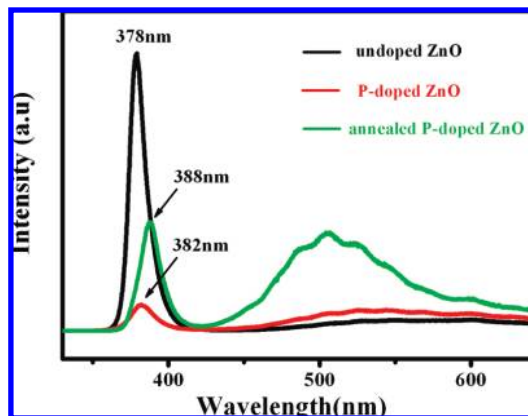


**Figure 3.** Room-temperature PL spectrum of the undoped ZnO nanorods and P-doped ZnO nanorods.

diffraction peak position of P-doped ZnO nanorods shifts to the large-angle side (as shown in the insert of Figure 2), which due to the P ions substitute the Zn sites in the crystal lattice to form  $P_{Zn}-2V_{Zn}$  complex defects.<sup>12,20</sup> This shift becomes larger for the annealed sample, which confirms P ion successfully diffused into the ZnO crystal lattice. The narrow full width at half-maximum (fwhm) of the (002) diffractive peak means after annealing the crystalline quality of P-doped ZnO nanorods could be improved.

Figure 3 shows the room-temperature PL spectra of undoped ZnO and P-doped ZnO. For the undoped ZnO nanorods the ultraviolet (UV) emission located at 378 nm is dominant in the PL spectrum, which is attributed to the near band gap excitonic emission. And the visible emission related to the defect in the crystal is weak. But for the doped sample the near band gap emission has a red-shift from 378 to 382 nm for the as-grown P-doped sample, to 388 nm for the annealed sample. And the emission intensity is weakened a lot. In addition, P-doped ZnO nanorods exhibit much stronger deep level emission. All these changes were considered due to the P doping in the ZnO crystal lattices.<sup>21</sup>

To further understand the origination of the ultraviolet emission of doped ZnO nanorods, the low-temperature PL spectra of undoped ZnO and P-doped ZnO were measured at 85 K as shown in Figure 4. The undoped ZnO nanorods show a strong near band edge emission located at 3.366 eV, which is assigned to a donor bound exciton ( $D^0X$ ; shown in Figure 4a). And the peak located at 3.233 eV is considered the phonon replicas of free exciton (FX). For the as-grown P-doped ZnO nanorods, the PL spectrum at 85 K is almost the same as the undoped one. But after the doped sample was annealed at high temperature, the P-doped sample showed three low-temperature emission peaks located at 3.364, 3.316, and 3.241 eV, respectively (as shown in Figure 4). The peak at 3.364 eV could be assigned to a donor bound exciton ( $D^0X$ ).<sup>22</sup> But the other two peaks located at 3.316 and 3.241 eV were not observed for the undoped sample. According to the previous reports of phosphorus-doped ZnO nanowires,<sup>14,23</sup> nitrogen,<sup>24</sup> and phosphorus-doped p-type ZnO thin films,<sup>20,25</sup> the origination of these two peaks is deduced related to acceptors in ZnO. The emission peaks at 3.316 and 3.241 eV are considered the recombination of free electron to the acceptor transition (FA) and the donor–acceptor pair (DAP) transition, respectively.<sup>14,23</sup> As shown in Figure 4b, with increasing temperature, the  $D^0X$  emission disappears at high temperature. But the FA and DAP emissions could be observed even at room temperature. The temperature-dependent PL spectra of annealed P-doped ZnO nanorods indicate the

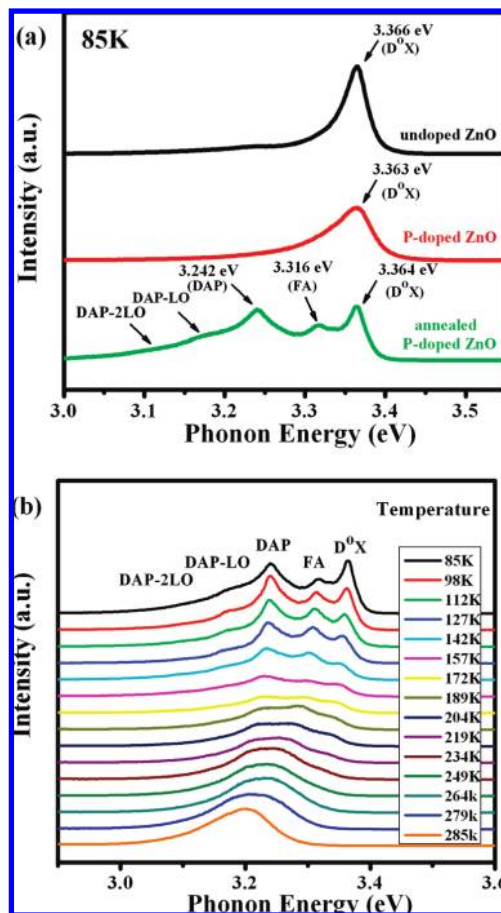
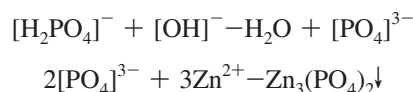


**Figure 4.** (a) Low-temperature PL spectra of undoped ZnO and P-doped ZnO and (b) temperature-dependent PL spectra of annealed P-doped ZnO.

origination of the room-temperature UV PL emission is a composite emission including DAP and FA.

On the basis of the above XRD and low-temperature PL analyses, we can deduce the P atoms have doped into the ZnO crystal lattice and formed an acceptor energy level. The P doping just occurred in the hydrothermal growth process. With an increase of the reaction temperature to 100 °C the concentration of  $[OH]^-$  increased, which induced the ZnO nanowire growth. At the same time the following reactions occurred:



The  $Zn_3(PO_4)_2$  deposition may be contained in ZnO nanorods during the nanorod growth process. After annealing,  $Zn_3(PO_4)_2$  was decomposed and the P atoms could diffuse into the ZnO crystal lattice serving as acceptor dopants. Referring to the theoretical and experimental reports about P doping in ZnO, it is deduced that the doped P ions may substitute the Zn sites in the ZnO lattice and form a complex acceptor as  $P_{Zn}-2V_{Zn}$ .<sup>12,20,26</sup>

To further prove the doping was efficient and the conductivity of P-doped ZnO nanorods may present a p-type, we constructed a ZnO nanorod homojunction fabricated by the hydrothermal method. The structure of the ZnO nanorods p–n homojunctions is schematically shown in Figure 5a. And the cross-section FESEM image shown in Figure 5b confirms this nanorod homojunction structure. Figure 5c shows the  $I-V$  curve of the device; the inset in Figure 5 shows the surface  $I-V$  characteristics of the n-type ZnO nanorods and P-doped ZnO nanorods

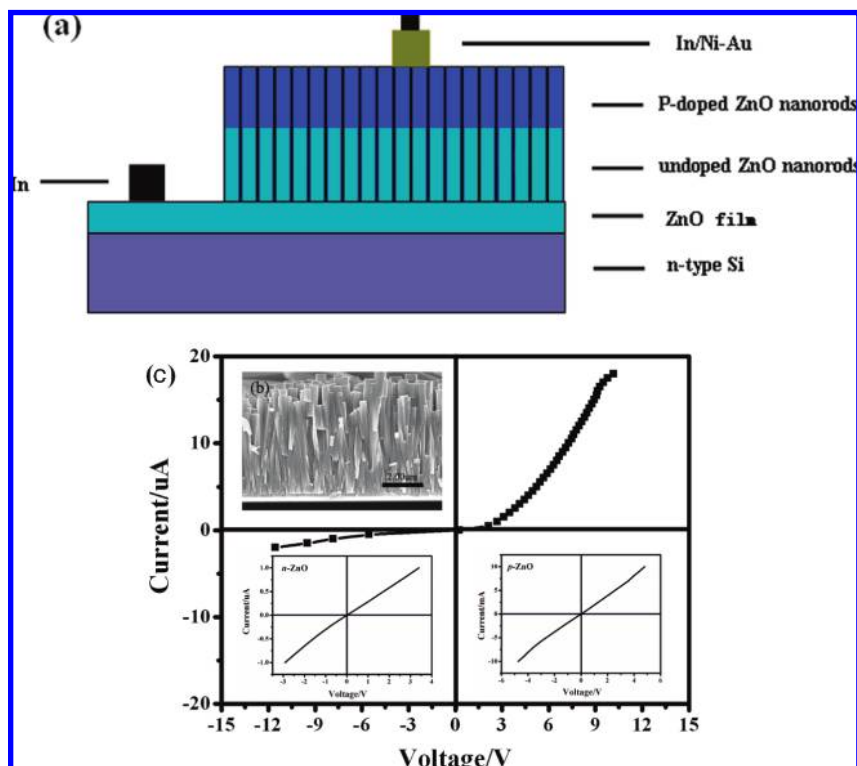


**Figure 5.** (a) Schematic of the ZnO nanorod p-n homojunction. (b) SEM cross-section image of the ZnO nanorod p-n homojunction. (c)  $I$ - $V$  curves for a p-n homojunction formed by p-type ZnO nanorods grown on n-type ZnO nanorods.

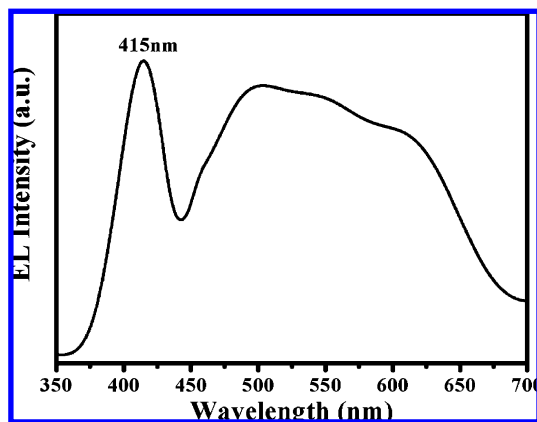


**Figure 6.** EL spectrum of the ZnO nanorod p-n homojunction.

in contact with the metal electrodes. The ohmic behaviors are confirmed by the fairly linear  $I$ - $V$  dependencies (shown in the insert of Figure 5c). The rectification behavior of the p-n junction is clearly displayed. The turn-on voltage appears at about 3.14 V under forward bias, and it is almost close to the band gap energy of ZnO. It is also found that the  $I$ - $V$  curve presents a little leakage current under reverse bias, and this could be due to incomplete contact between some nanorods and the contact metal electrode. The  $I$ - $V$  characteristics of ZnO nanorod p-n homojunctions proves the hydrothermal-grown P-doped ZnO nanorods may have the p-type conductivity, which is valuable for fabricating ZnO nanorods light emission diodes.

The EL measurement of the ZnO nanorod p-n homojunction was performed at room temperature, and the results are shown in Figure 6. When the inject current is 7 mA, the spectrum exhibits two independent EL bands: a near-band-edge emission (NBE) at 415 nm and a broad visible emission band ranging from 450 to 650 nm. The origination of the emission peak

located at 415 nm is contributed to the donor-acceptor recombination in the P-doped ZnO nanorods. And the broad visible emission band is due to the defect related radiated recombination.<sup>16</sup>

## Conclusions

In conclusion, P-doped ZnO nanorods and ZnO nanorod p-n homojunctions were synthesized by the hydrothermal method. The XRD and low-temperature PL spectra measurements have confirmed the P atoms doped into the ZnO crystal lattice and formed an acceptor energy level. With construction of 1D ZnO nanostructure p-n homojunctions, the  $I$ - $V$  curve showed typical rectification characteristics of p-n junctions with a turn-on voltage of about 3.14 V, which implied the P-doped ZnO nanorods might be of p-type conductivity. Furthermore, the EL spectrum was obtained on this ZnO nanorod p-n homojunction at room temperature with a violet-blue emission band centered at 415 nm and a broad visible band. The above result demonstrated the hydrothermal method was an efficient p-type doping method for fabricating P-doped ZnO nanorods and ZnO-based 1D LED. One promising advantage for this method was no special requirement for the substrate.

**Acknowledgment.** This work is supported by the Key Project of the National Natural Science Foundation of China under Grant No. 50532050, the "973" program under Grant No. 2006CB604906, the Innovation Project of the Chinese Academy of Sciences, the National Natural Science Foundation of China under Grant Nos. 60429403, 60506014, 50402016, 10674133, 10647105, and 60670659, the Project of Science Development Planning of Jilin Province (Grant 0070519), and the Program for New Century Excellent Talents in University (Grant NCET-07-022).

## References and Notes

- (1) Shan, C. X.; Liu, Z.; Hark, S. K. *Appl. Phys. Lett.* **2008**, *92*, 073103.
- (2) Jiao, S. J.; Zhang, Z. Z.; Lu, Y. M.; Shen, D. Z.; Yao, B.; Zhang, J. Y.; Li, B. H.; Zhao, D. X.; Fan, X. W.; Tang, Z. K. *Appl. Phys. Lett.* **2006**, *88*, 031911.
- (3) Heo, Y. W.; Kwon, Y. W.; Li, Y.; Pearton, S. J.; Norton, D. P. *Appl. Phys. Lett.* **2004**, *84*, 3474.
- (4) Sun, J. C.; Zhao, J. Z.; Liang, H. W.; Bian, J. M.; Hu, L. Z.; Zhang, H. Q.; Liang, X. P.; Liu, W. F.; Du, G. T. *Appl. Phys. Lett.* **2007**, *90*, 121128.
- (5) Mandalapu, L. J.; Xiu, F. X.; Yang, Z.; Zhao, D. T.; Liu, J. L. *Appl. Phys. Lett.* **2006**, *88*, 112108.
- (6) Wu, J. J.; Liu, S. C.; Wu, C. T.; Chen, K. H.; Chen, L. C. *Appl. Phys. Lett.* **2002**, *81*, 1312.
- (7) Kong, X. Y.; Ding, Y.; Wang, Z. L. *J. Phys. Chem. B* **2004**, *108*, 570.
- (8) Yang, P. D.; Yan, H. Q.; Mao, S.; Russo, R.; Johnson, J.; Saykally, R.; Morris, N.; Pham, J.; He, R.; Choi, H. J. *Adv. Funct. Mater.* **2002**, *12*, 323.
- (9) Vayssieres, L. *Adv. Mater.* **2003**, *15*, 464.
- (10) Ma, D. D. D.; Lee, C. S.; Au, F. C. K.; Tong, S. Y.; Lee, S. T. *Science* **2003**, *299*, 1874.
- (11) Tong, Y. H.; Liu, Y. C.; Dong, L.; Lu, L. X.; Zhao, D. X.; Zhang, J. Y.; Lu, Y. M.; Shen, D. Z.; Fan, X. W. *Mater. Chem. Phys.* **2007**, *103*, 190.
- (12) Xiang, B.; Wang, P. W.; Zhang, X. Z.; Dayeh, S. A.; Aplin, D. P. R.; Soci, C.; Yu, D. P.; Wang, D. L. *Nano Lett.* **2007**, *7*, 323.
- (13) Cao, B. Q.; Lorenz, M.; Rahm, A.; Wenckstern, H. V.; Zekalla, C. C.; Lenzner, J.; Benndorf, G.; Grundmann, M. *Nanotechnology* **2007**, *18*, 455707.
- (14) Shan, C. X.; Liu, Z.; Wong, C. C.; Hark, S. K.; Nanosci, J. *Nanotechnology* **2007**, *7*, 700.
- (15) Zhang, J. Y.; Li, P. J.; Sun, H.; Shen, X.; Deng, T. S.; Zhu, K. T.; Zhang, Q. F.; Wu, J. L. *Appl. Phys. Lett.* **2008**, *93*, 021116.
- (16) Sun, M.; Zhang, Q. F.; Wei, J. L. *J. Phys. D: Appl. Phys.* **2007**, *40*, 3798.
- (17) Sun, X. W.; Huang, J. Z.; Wang, J. X.; Xu, Z. *Nano Lett.* **2008**, *8*, 1219.
- (18) Hsu, Y. F.; Xi, Y. Y.; Tam, K. H.; Djuricic, A. B.; Luo, J.; Ling, C. C.; Cheung, C. K.; Ng, A. M. C.; Chan, W. K.; Deng, X.; Beling, C. D.; Fung, S.; Cheah, K. W.; Fong, P. W. K.; Surya, C. C. *Adv. Funct. Mater.* **2008**, *18*, 1020.
- (19) Vaithianathan, V.; Lee, B. T.; Kim, S. S. *J. Appl. Phys.* **2005**, *98*, 043519.
- (20) Qin, R.; Zheng, J. X.; Lu, J.; Wang, L.; Lai, L.; Luo, G. F.; Zhou, J.; Li, Hong.; Gao, Z. X.; Li, G. P.; Mei, W. N. *J. Phys. Chem. C*, in press.
- (21) Hsu, C. L.; Chang, S. J.; Lin, Y. R.; Tsaib, S. Y.; Chen, I. C. *Chem. Commun. (Cambridge)* **2005**, 3571.
- (22) Xiu, F. X.; Yang, Z.; Mandalapu, L. J.; Liu, J. L.; Beyermann, W. P. *Appl. Phys. Lett.* **2006**, *88*, 052106.
- (23) Hwang, D. K.; Kim, H. S.; Lim, J. H.; Oh, J. Y.; Yang, J. H.; Parka, S.; Ju.; Kim, K. K.; Look, D. C.; Park, Y. S. *Appl. Phys. Lett.* **2005**, *86*, 151917.
- (24) Yang, X. D.; Xu, Z. Y.; Sun, Z.; Sun, B. Q.; Ding, L.; Wang, F. Z.; Ye, Z. Z. *J. Appl. Phys.* **2006**, *99*, 046101.
- (25) Xiu, F. X.; Yang, Z.; Mandalapu, L. Z.; Liu, J. L. *Appl. Phys. Lett.* **2006**, *88*, 152116.
- (26) Park, C. H.; Zhang, S. B.; Wei, S. H. *Phys. Rev. B* **2002**, *66*, 073202.

JP906175X